View metadata, citation and similar papers at core.ac.uk

brought to you by CORE

provided by Scholarship@Claremont

Claremont Colleges
Scholarship @ Claremont

All HMC Faculty Publications and Research | HMC Faculty Scholarship

9-1-2006

In Situ Muscle Power Differs Without Varying In Vitro Mechanical Properties in Two Insect Leg Muscles Innervated by the Same Motor Neuron

Anna N. Ahn
Harvey Mudd College

Kenneth Meijer
University Maastricht

Robert J. Full
University of California - Berkeley

Recommended Citation

Ahn, AN, Meijer, K, Full, RJ. In situ muscle power differs without varying in vitro mechanical properties in two insect leg muscles innervated by the same motor neuron. J Exp Biol. 2006;209(17): 3370-3382.

This Article is brought to you for free and open access by the HMC Faculty Scholarship at Scholarship @ Claremont. It has been accepted for inclusion in All HMC Faculty Publications and Research by an authorized administrator of Scholarship @ Claremont. For more information, please contact scholarship@cuc.claremont.edu.

The Journal of Experimental Biology 209, 3370-3382
Published by The Company of Biologists 2006
doi:10.1242/jeb.02392

In situ muscle power differs without varying *in vitro* mechanical properties in two insect leg muscles innervated by the same motor neuron

A. N. Ahn*, K. Meijer† and R. J. Full

Department of Integrative Biology, University of California, Berkeley, CA 94720-3140, USA

*Author for correspondence at present address: Department of Biology, Harvey Mudd College, 301 Platt Boulevard, Claremont, CA 91711, USA (e-mail: aahn@hmc.edu)

†Present address: Movement Science Group, Department of Health Sciences, University Maastricht, PO Box 616, 6200 MD, Maastricht, The Netherlands

Accepted 18 June 2006

Summary

The mechanical behavior of muscle during locomotion is often predicted by its anatomy, kinematics, activation pattern and contractile properties. The neuromuscular design of the cockroach leg provides a model system to examine these assumptions, because a single motor neuron innervates two extensor muscles operating at a single joint. Comparisons of the *in situ* measurements under *in vivo* running conditions of muscle 178 to a previously examined muscle (179) demonstrate that the same inputs (e.g. neural signal and kinematics) can result in different mechanical outputs. The same neural signal and kinematics, as determined during running, can result in different mechanical functions, even when the two anatomically similar muscles possess the same contraction kinetics, force–velocity properties and tetanic force–length properties. Although active shortening greatly depressed force under *in vivo*-like strain and stimulation conditions, force depression was similarly proportional to strain, similarly inversely proportional to stimulation level, and similarly independent of initial length and shortening velocity between the two muscles. Lastly, passive pre-stretch enhanced force similarly between the two muscles. The forces generated by the two muscles when stimulated with their *in vivo* pattern at lengths equal to or shorter than rest length differed, however. Overall, differences between the two muscles in their submaximal force–length relationships can account for up to 75% of the difference between the two muscles in peak force generated at short lengths observed during oscillatory contractions. Despite the fact that these muscles act at the same joint, are stimulated by the same motor neuron with an identical pattern, and possess many of the same *in vitro* mechanical properties, the mechanical outputs of two leg extensor muscles can be vastly different.

Key words: muscle, work loop, motor control.

Introduction

The nervous system generates electrical signals that activate the locomotor muscles of an animal to produce movements like running, flying and swimming. Along with kinematics, the timing and duration of these electrical signals, and the contractile properties of the muscles (e.g. contraction kinetics, force–velocity relationship, tetanic force–length characteristics and history-dependent properties) are often considered to be the determinants of muscle function (for reviews, see Josephson, 1999; Dickinson et al., 2000). In the present study, we examine whether any of these determinants sufficiently predict the mechanical function of muscle during locomotion.

The neuromuscular design of the cockroach leg provides a model system to investigate the neural control and mechanical function of multiple muscles during locomotion, because two extensor muscles operating at the same joint are innervated by a single motor neuron. In a previous study, two muscles within the multiple muscle system of this cockroach leg were found to function differently, where one muscle functions like a motor (muscle 177c) and the other muscle functions like a brake (muscle 179) under *in vivo* running conditions (Ahn and Full, 2002). Although both muscles consist of fast-twitch muscle fibers, the two muscles operate at different regions of their relative force–velocity relationships because the rest length of muscle 177c measured more than twice that of muscle 179 (Ahn and Full, 2002). To test whether the anatomy, muscle activity patterns, kinematics and *in vitro* contractile properties of a muscle sufficiently predict its mechanical function in the present study, we performed a series of experiments on two locomotory muscles of similar length innervated by a single motor neuron (178 and 179) (Carbonell, 1947). These two anatomically distinct muscles technically constitute a single motor unit (Fig. 1) (Usherwood, 1962; Pipa and Cook, 1959) and are positioned to generate extensor torques at the

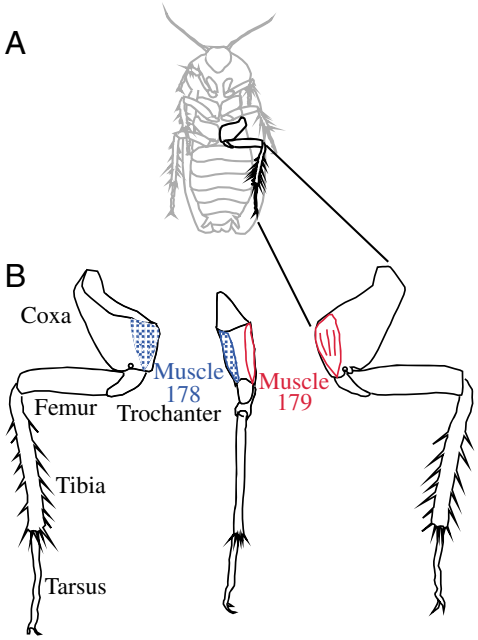

Fig. 1. Musculo-skeletal morphology of the hindlimb and muscles of interest. (A) Ventral view of the cockroach with the left hindleg in bold. (B) Dorsal, medial and ventral views (from left to right, respectively) of the left hindlimb. Muscle 178 (blue, shaded) inserts on the trochanter and originates on the dorsal side of the coxa closest to the body. The center image represents lateral view from the midline of the animal to clearly show the positions of the muscles. Muscle 179 (red, unshaded) inserts on the trochanter and originates on the ventral side of the coxa. Note that the moment arms are similar between the muscles, but muscle 178 is slightly shorter in length (see Table 1) and slightly broader with greater cross-sectional area. The circles in the dorsal and ventral views of the hindlimb indicate the axis of rotation of the joint.

coxal–trochanteral–femoral joint of the hindlimb of the cockroach, *Blaberus discoidalis.* As a group, the extensors of the hindlimb produce power to extend the leg and accelerate the center of mass forward during running (Full et al., 1991). Homologues of both muscles are ultrastructurally similar and histochemically classified as fast-twitch muscles in a related species, the American cockroach *Periplaneta americana* (Stokes et al., 1979; Morgan et al., 1980; Stokes, 1987). For this study, we begin by testing the null hypothesis that muscles 178 and 179 function similarly under *in vivo* conditions.

To test our hypothesis, we use the *in situ* 'work loop' technique to measure their net mechanical energy and determined their mechanical function during cyclical contractions (Josephson, 1985). The *in vivo* strain and stimulation conditions determined during running are imposed on the muscles. Some data for muscle 179 have been previously reported (Full et al., 1998; Ahn and Full, 2002). These previously reported data are indicated and are presented in the current manuscript only to provide clear, direct comparisons with data from muscle 178. Despite their similar anatomical positions and moment arm relationships with joint angle (Full and Ahn, 1995), muscles 178 and 179 differ slightly in length. Therefore, the *in vivo* strain amplitudes differ slightly between the two muscles, even though the other aspects of their strain and stimulation patterns are identical. To examine the effects of strain amplitude on power ouptut, we also examine the mechanical function of the muscles when operating under identical strain conditions. Subsequently, to explain any differences in mechanical function, we compare both commonly and less frequently examined intrinsic properties of the two muscles, including isometric contraction kinetics, force–velocity characteristics, tetanic and submaximal force–length properties, force depression due to active shortening, and force enhancement due to passive lengthening.

Materials and methods

Animals and muscles

Blaberus discoidalis L. cockroaches were obtained from a commercial supplier (Carolina Biological Supply Co., Gladstone, OR, USA). The animals were maintained in the laboratory in large, enclosed containers where they had free access to dried dog food and water. The following, previously unpublished experiments used 94 animals (mass=2.76±0.69 g; mean ± s.d.). Some animals were used in only one type of experiment (e.g., muscle power or force–velocity), while other animals were used in multiple types of experiments.

The muscles selected for study, muscles 178 and 179 of the cockroach hindlimb (see Carbonell, 1947), are positioned to extend the coxal–trochanteral–femoral joint and depress the femur (Fig. 1). Muscle 178 originates on the dorsal wall and rim of the coxa and inserts on a small apodeme that extends from the dorsal, proximal end of the trochanter. Muscle 179 originates on the ventral wall and rim of the coxa and inserts on a small apodeme that extends from the ventral, proximal end of the trochanter. Both mono-articular muscles have similar moment arm relationships with the coxal–trochanteral–femoral joint angle (Full and Ahn, 1995). In our study, we ignore the small movements of the trochanteral–femoral joint, as in previous studies (Full and Ahn, 1995; Full et al., 1998). The trochanteral–femoral joint has a very small range of dorso-ventral motion, which is orthogonal to the anterio-posterior motion of the coxal–trochanteral joint. Therefore, movements in the trochanteral–femoral joint do not affect the strain of muscles 178 and 179.

In vivo muscle activity patterns

For the *in vivo* muscle activity pattern of muscle 178, we used the electromyographical (EMG) patterns of muscle 179 obtained during running in a previous experiment (Ahn and Full, 2002) because the same, single, excitatory motor neuron innervated both muscles (Pipa and Cook, 1959) with no inhibitory innervation (Pearson and Iles, 1971). To ensure that the activation pattern of muscle 178 can be assumed from the EMG recordings of muscle 179 during running, we measured EMG recordings from both muscles under two controlled conditions. The first ('*in vivo*') condition allowed the animal to activate its muscles while constrained on a custom-made Lucite

chamber with all nerves intact. In response to gentle contact, the animal freely activated muscles 178 and 179, from which EMG signals were recorded. In the second ('*in situ*') condition, we severed the nerve from the metathoracic ganglion and directly stimulated the motor neuron at varying frequencies while recording EMG signals from both muscles. A stimulation isolation unit (SIU 90; NeuroData Instruments Corp., New York, NY, USA) injected bursts of current at frequencies of 1 to 150 Hz through a suction electrode *via* Nerve 5. A stimulator (S48 stimulator; Grass Instruments, Quincy, MA, USA) controlled the bursts of stimulation. The muscle action potentials merged at stimulation frequencies higher than 150 Hz, causing individual motor action potentials to be indiscernible from one another.

All EMG recordings were acquired at 3 kHz (Labview DAQ system; NI PCI-1200 boards; National Instruments, Austin, TX, USA) on a computer (Macintosh Power PC 9500/132). Muscle action potentials recorded from muscles 178 and 179 were amplified 100 times at a bandwidth of 3 Hz to 1 kHz (P5 series A.C. pre-amps; Grass Instruments, Quincy, MA, USA). Bipolar electrodes were made from 50 μm (44 gauge) silver wire insulated with polyurethane (California Fine Wire, Grover Beach, CA, USA) (for details, see Full et al., 1998; Ahn and Full, 2002). We ensured the lack of electrical crosstalk by recording signals from both pairs of electrodes, while only one pair of electrodes was inserted into a muscle. If muscle action potentials were observed only from the electrodes implanted into a muscle, then we concluded that electrical crosstalk was minimal and then implanted the second pair of electrodes into the other muscle.

In vivo muscle strain patterns

For the strain change pattern of muscle 178, we used the kinematics determined from digitizing points (Motus, Peak Performance Technologies, Inc., Colorado Springs, CO, USA) on the hindlimb joints of a running animal recorded with high-speed video (500 frames s^{-1}, Redlake Camera Systems, Tucson, AZ, USA). The joint kinematics were played into a three-dimensional musculo-skeletal model of the cockroach hindlimb (SIMM, MusculoGraphics, Inc, Santa Rosa, CA, USA) (Full and Ahn, 1995). Muscle strain correlates tightly with joint angle in insect legs because these muscles insert onto apodemes (i.e. arthropod 'tendon'), which are 40 times stiffer than vertebrate tendon (Ker, 1977; Full et al., 1998).

In situ muscle measurements

For all *in situ* muscle measurements, animals were chilled and restrained with a custom-made Lucite chamber. Details of the setup were as described (Full et al., 1998; Ahn and Full, 2002). The Lucite chamber restrained the body, fore- and midlegs of the animal while quick-setting epoxy held the hindlimbs fixed. We then isolated the distal end of the muscle of interest. Muscle 178 lay most dorsal, or deepest when the animal was fixed dorsal-side down, within the coxal segment of the cockroach hindlimb (Fig. 1). Muscle 178 was isolated by carefully removing the ventral exoskeleton of the hindlimb coxa and dissecting away the other extensor muscles (177a, 177c, 177d, 177e and 179). Rest length (*RL*), defined as the length of the muscle when the coxal–trochanteral–femoral joint was positioned at a 90° angle, was carefully measured with an ocular micrometer. A small piece of the trochanteral exoskeleton connected to the 178 apodeme was cut and was then inserted into a stainless steel hook on the servo lever arm. In contrast, muscle 179 lay most ventral within the coxal segment of the hindlimb (Fig. 1). Details of the dissection for muscle 179 were as previously reported (Full et al., 1998; Ahn and Full, 2002). Some data for muscle 179 have been previously reported (Full et al., 1998; Ahn and Full, 2002). These previously reported data are indicated and are presented in the current manuscript only to provide clear, direct comparisons with data from muscle 178.

A dual-mode muscle lever system obtained forces while simultaneously controlling lengths of the muscles (model 300B; Cambridge Technology, Inc., Cambridge, MA, USA). *In situ* forces were acquired with a computer program (Labview, National Instruments, Austin, TX, USA), which controlled muscle length while measuring muscle force or controlled muscle force while measuring muscle length. The distal apodeme was attached to a small hook on the lever arm of the servo motor system. The muscle was stimulated (S48 stimulator; Grass Instruments, Quincy, MA, USA) with a suction electrode on Nerve 5, which contains the motor neuron (Pearson and Iles, 1971). The stimulation consisted of 0.5 ms square-wave pulses at approximately twice the threshold voltage, or the minimum voltage that elicited a twitch contraction. 2 min rests separated the trials that used submaximal stimulation, or the *in vivo* '3s' (3 pulses at 100 Hz), stimulation pattern (Full et al., 1998; Ahn and Full, 2002) and 5 min rests separated the trials that used tetanic stimulation. Maintenance of muscle performance was periodically checked with isometric contractions when the muscle was stimulated with the *in vivo* 3s pattern. These isometric contractions were the simplest tests of muscle performance. The experiment was stopped when muscle performance declined by more than 10% of its original force. The dissected area was periodically moistened with insect saline (Becht et al., 1960). All *in situ* muscle measurements were performed at 25±1°C.

Work loop technique

The area of the loop formed by plotting muscle force as a function of muscle length equaled the work or energy per cycle (Josephson, 1985). For each trial, the *in vivo* strain and stimulation patterns were imposed to obtain four cyclical contractions. Net *in situ* power per cycle was calculated by dividing net *in situ* work of the third cycle by the cycle period.

The *in vivo* strain and stimulation parameters used during the *in situ* work loop experiments were obtained from the animals running at their preferred speed [approximately 24 cm s^{-1}, cycle frequency of 8 Hz (Full et al., 1998; Ahn and Full, 2002)]. The imposed muscle parameters included the muscle strain pattern (trajectory, amplitude and cycle

frequency) and the stimulation pattern (phase, frequency and burst duration) as determined during running in previously published experiments (Full et al., 1998; Ahn and Full, 2002). The *in vivo* activation pattern for muscle 179 occurred near the beginning of the stance phase (phase 26%, where 0% represents midway through lengthening) and consisted of the 3s pattern, or a burst of three muscle action potentials at 100 Hz. To examine the effect of strain amplitude on muscle power, we systematically varied strain amplitude while keeping all other aspects of the strain and stimulation patterns constant. For our study, strain was calculated by dividing the change in length from *RL* by *RL*. Multiplying this by 100 equaled the percentage strain, where a positive strain represented muscle lengths longer than *RL* and a negative strain represented muscle lengths shorter *RL*.

Kinetics of isometric contractions

The kinetics of isometric contraction included the time to peak force (T_{max}), time to 50% relaxation (T_{50off}), and time to 90% relaxation (T_{90off}). These times began at the onset of stimulation (T=0) to most closely represent the time between muscle stimulation and force generation *in vivo*. The times measured, therefore, include the latency periods or the time between the onset of stimulation and the onset of force generation. For a twitch contraction, the muscle was stimulated with a single pulse of stimulation. For a contraction using the *in vivo* activation pattern, the muscle was stimulated with *in vivo* 3s pattern. All muscles were held isometrically at *RL*.

Force–velocity relationships

The force–velocity relationship of muscle 178 was determined using the force-clamp method (Edman, 1979). Tetanically stimulated muscles were shortened isotonically at varying force levels. The velocity of shortening was determined for each force level over a 5 ms interval at the beginning of constant shortening. For each individual, the maximum shortening velocity (V_{max}) for muscle 178 was determined by extrapolation of the force–velocity measurements to zero force. The Hill constants and V_{max} were determined using the least-squares method (Wohlfart and Edman, 1994). The Hill coefficients were then averaged to obtain the overall, average Hill coefficients that represent the force–velocity relationship for muscle 178. These methods were similar to those used to determine the force–velocity relationship of muscle 179, which have been previously published (Ahn and Full, 2002).

Tetanic force–length relationships

The force–length relationships of the two muscles were determined using tetanic bursts of stimulation (200 Hz for 200 ms), while the muscles were held isometrically. This tetanic stimulation pattern was also used in a previous study to examine tetanic force generation at *RL* in muscle 179 (Full et al., 1998). For the current study, muscle length was varied randomly for each trial. The muscle was set at the prescribed length for at least 1 min before data collection to allow the viscoelastic properties of the muscle to settle at the new length. Optimal length, or the length at which force was maximal, was determined by fitting a second-order polynomial to the data for each individual. The coefficients of the binomial fits were averaged to obtain the overall, or average, binomial fit for muscles 178 and 179. Zero strain represented *RL*, defined as the length of the muscle when the coxal–trochanteral–femoral joint was set at 90° (Full et al., 1998). We assumed *RL* for muscle 178 occurred at the 90° joint angle because this joint angle determined the *RL* for muscle 179 (Ahn and Full, 2002). The muscles were rested for 5 min between trials, unless the maximum tetanic force declined during a contraction performed at *RL*. When the muscle began to fatigue, a longer inter-trial time allowed for a more complete recovery. If the maximum tetanic force continued to decline or if muscle force declined by more than 10% of its original force at *RL*, the experiment was stopped.

Submaximal force–length relationships

The force–length relationships of the two muscles were determined using the *in vivo* 3s stimulation pattern measured during running [3 pulses at 100 Hz (Full et al., 1998; Ahn and Full, 2002)]. For each trial, muscle length was varied randomly. The muscle was set at the prescribed length at least 1 min before data collection to allow the viscoelastic properties of the muscle to settle at the new length. Again, zero strain represented *RL*. The length at which maximum force was generated could not be determined at the 3s stimulation level because forces generated were usually maximal at the longest lengths examined. Lengths longer than +10% strain were not examined because muscle performance typically declined, possibly due to damage. Therefore, 'optimal length' referred to the length at which maximum force was generated during tetanic contractions.

Force depression due to active shortening

Force depression due to active shortening may play an important role in determining muscle force generation *in vivo* since these muscles were activated at the beginning of the stance phase of running as the muscles began shortening (Fig. 2). Similar to previous studies, force depression due to active shortening was determined as the percentage difference between the peak force of a contraction with active shortening and the peak force of an isometric contraction held at the final, shortened length (Edman, 1975). This isometric contraction measured at the final shorter length without a previous shortening served as the control. The muscles were shortened as force developed during the contraction 25 ms after the onset of stimulation. A sufficiently high shortening velocity (100 mm s^{-1}) prevented force generation during shortening (Edman, 1975). The default parameters included 100 mm s^{-1} shortening velocity, 2.5% (or 0.5 mm) shortening strain, 3s stimulation pattern, and 0 initial length (i.e. *RL*). While examining the effect of one variable, the other variables were set to the default parameters. These varied parameters consisted of shortening velocity (15 mm s^{-1}, 50 mm s^{-1}, 100 mm s^{-1},

200 mm s^{-1}), shortening distance or strain (0.1, 0.2, 0.3 mm, or until force was undetectable), initial length (*RL*, *RL*+0.1 mm, *RL*+0.2 mm), and stimulation duration (1–4 pulses of stimulation at 100 Hz). The ranges of the parameters examined for muscles 178 and 179, respectively, included the *in vivo* or as close as possible to the *in vivo* ranges of strains (0.65 mm and 0.67 mm), shortening velocities (14.3 mm s^{-1} and 15.2 mm s^{-1}), and stimulation levels (3s) observed in the animal during running (Full et al., 1998; Ahn and Full, 2002).

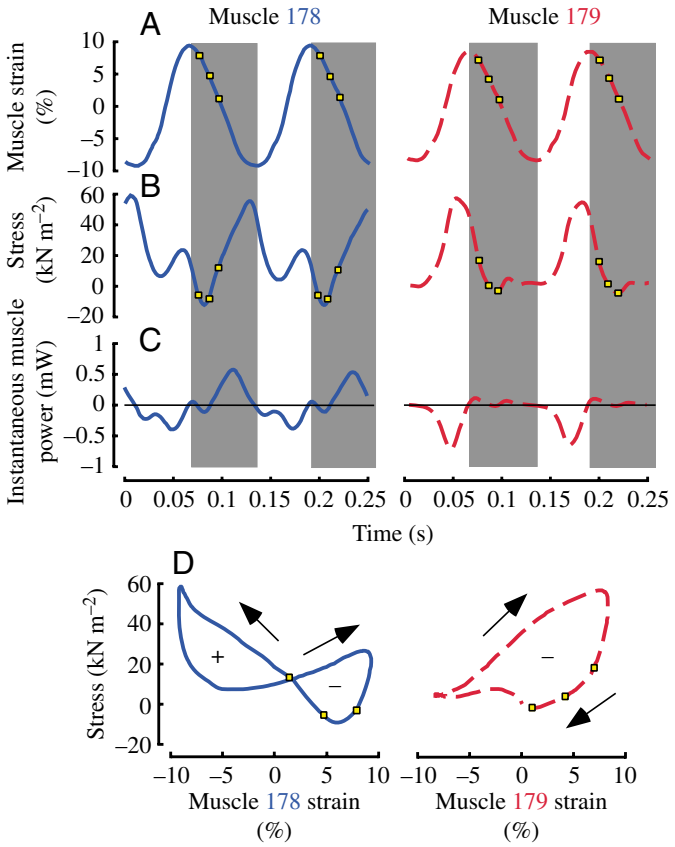

Fig. 2. Representative strain, total stress and power when muscles 178 and 179 operated under *in vivo* strain and stimulation conditions. The shaded area represents the shortening phase of the oscillatory cycle. The stimulation pattern, represented on the graphs by the yellow squares, was also determined during running at the animal's preferred speed (3 pulses at 100 Hz) (Full et al., 1998; Ahn and Full, 2002). (A) The strain pattern as determined during preferred speed running. Since muscle 178 is slightly shorter in length, 178 experiences slightly longer strain amplitudes (18.5% for muscle 178, 16.4% for muscle 179). (B) *In situ* muscle stress during imposed running conditions. The shaded areas represent the shortening (or stance) phase of the oscillatory cycle. (C) Instantaneous muscle power during running. Muscle 178 absorbs energy during lengthening, while generating power during the shortening phase. Muscle 179 also absorbs energy during lengthening, but did not generate power during the shortening phase. (D) Work loops for muscles 178 and 179 under *in vivo* conditions. Work loops show that muscle 178 generated no net mechanical power over the cycle, while muscle 179 absorbed net mechanical power over the cycle. The arrows indicate the directions of the loops. The dominant clockwise work loop for muscle 179 illustrates that this muscle generated higher forces during lengthening than during shortening, resulting in negative work or mechanical energy absorption when operating under the conditions experienced during preferred speed running. These data for muscle 179 were previously reported (Full et al., 1998; Ahn and Full, 2002), and are presented to allow direct comparison to the data of muscle 178.

Force enhancement due to passive pre-stretch

Force enhancement due to a passive pre-stretch may play an important role in determining muscle force generation *in vivo* because these muscles are passively stretched during the swing phase prior to the stance phase of running (muscle shortening) and the onset of activation (Fig. 2). We measured force enhancement due to passive pre-stretch by quantifying the percentage difference between the peak force of a muscle contraction with a passive pre-stretch and the peak force of an isometric contraction held at the longer, final length. The isometric contraction measured at the longer length without a pre-stretch served as the control. The default parameters were 0.5 mm (10–13%) pre-stretch at 15 mm s^{-1}, 3s stimulation pattern, and 1 ms pause period (i.e., stimulation occurred 1 ms after the pre-stretch ended). The parameters varied included pre-stretch distance (0.2, 0.4, 0.5, 0.6, 0.7, 0.8 mm), velocity of pre-stretch (5, 10, 15, 100 mm s^{-1}), and stimulation level (1–4 pulses of stimulation at 100 Hz). The ranges of the parameters examined included the *in vivo* ranges of strains, shortening velocities and stimulation levels, as observed in the animal during running.

Statistics

All data were calculated as mean ± s.d. To avoid pseudo-replication, each animal generated a single data point for all data sets. When repeated measures existed from any animal, the values were averaged to represent that animal under those conditions. Comparisons were made between data for muscles 178 and 179 using Student's unpaired *t*-tests or analyses of covariance (ANCOVA) to give *P*-values (Statview 5.0, Cary, NC, USA). An ANCOVA was used to determine differences in force depression due to active shortening and force enhancement due to passive lengthening between the two muscles. For an ANCOVA, the dependent variable was the history-dependent property, the independent variables or covariates included shortening strain, initial length, shortening velocity, stimulation level, magnitude of passive pre-stretch and velocity of passive pre-stretch, and the factor examined was the muscle (178 or 179). Differences were considered statistically significant when $P<0.05$.

Results

Sample set

In situ muscle measurements were obtained from 109 animals (mass=2.82±0.70 g). The average mass of the animals used for experiments on muscle 178 (mass=2.70±0.63 g; *N*=53 animals) was similar to the average mass of the animals used for experiments on muscle 179 (mass=2.93±0.76 g; *N*=56;

$P>0.05$). The average length of muscle 178 (3.51±0.23 mm; $N=53$ animals) was 8.3% shorter than that of muscle 179 (3.99±0.27 mm; $N=56$ animals; $P<0.0001$).

Delay of electrical activity between muscles

Both muscles received signals from the motor neuron simultaneously when the animal activated its muscles (*in vivo*) and when the motor nerve was stimulated at varying frequencies (*in situ*). When stimulated through the nerve, the time interval between the EMG signals of the two muscles did not differ from zero at all frequencies (range=–0.61–0.54 ms; $P>0.3$ for all frequencies). Moreover, the delay of activity between the muscles when current was injected into the nerve was independent of stimulation frequency ($P=0.88$; $N=9$ animals; mass=2.65±0.51 g), and both muscles always received simultaneous stimulation or neither muscle received stimulation during all trials.

In situ muscle measurements

Muscle power under in vivo conditions

In vivo neural inputs and kinematic patterns imposed on the two anatomically similar muscles resulted in dissimilar muscle function (Fig. 2). During simulated running, muscle strain amplitude was determined to be 18.5% for muscle 178. Under these *in vivo* conditions, muscle 178 both produced and absorbed energy to result in near zero net mechanical energy production during a cycle (1.79±4.58 W kg^{-1}; $N=6$; $P=0.4$). In contrast, muscle 179 absorbed net mechanical energy during each cycle, as previously shown (–19.1±14.1 W kg^{-1}; $N=6$) (Full et al., 1998; Ahn and Full, 2002). The main difference between the two muscles consisted of the force generated during shortening, since both muscles absorbed energy during lengthening (Fig. 2B,C). In muscle 178, force peaked shortly after the onset of stimulation, then declined before the onset of lengthening. In contrast, muscle 179 did not generate force during shortening, but rather generated force only during the lengthening phase of the cycle. Furthermore, the mechanical energies absorbed during passive, cyclical contractions were similar between the two muscles (Table 1).

Muscle power varied with strain amplitude

Although the magnitude of power differed between the two muscles, net power per cycle decreased similarly with increasing strain amplitude in both muscles (Fig. 3; $P=0.73$ for averaged slopes; $P<0.001$ for y-intercepts). With respect to work loop shape, the positive, energy-producing portion of the cycle diminished in size while the negative, energy-absorbing portion of the cycle expanded with increasing strain amplitude (Fig. 3). In muscle 178, the mechanical energy generated during shortening exceeded the energy absorbed during lengthening at most strain amplitudes. However, at the greatest strain amplitudes (>18.5%), the energy produced during shortening by muscle 178 closely matched the energy absorbed during lengthening, resulting no net mechanical energy production or

Table 1. *Mechanical properties of muscles 178 and 179*

	178	*N*	179	*N*	*P*
Twitch kinetics (ms)					
T_{max}	30.4±1.6	7	26.5±4.8*	8	0.1
T_{50off}	42.7±1.8	7	39.5±6.2*	8	0.3
T_{90off}	64.5±5.0	7	60.2±7.6*	8	0.4
3s contraction kinetics (ms)					
T_{max}	46.8±1.1	6	46.8±5.3*	8	0.2
T_{50off}	65.6±1.5	6	61.7±7.6*	8	0.6
T_{90off}	82.0±5.2	6	76.3±9.9*	8	0.5
Optimal length (% of *RL*)	108±2	5	111±3	5	0.18
V_{max} (mm s^{-1})	19.9±3.8	5	20.6±3.0*	5	0.76
V_{max} (*L* s^{-1})	5.6±0.7	5	4.9±0.4*	5	0.11
Maximum *in vivo* velocity (*L* s^{-1})†	4.1±0.1	6	3.7±0.1	6	<0.01
Muscle length (mm)	3.5±0.3	6	4.1±0.3*	6	<0.01
Muscle mass (mg)	4.0±0.8	6	3.2±0.5	6	<0.01
Total work per cycle (J kg^{-1})†	0.014±0.28	6	–2.4±1.8*	6	<0.01
Total power per cycle (W kg^{-1})†	1.97±4.49	6	–19.1±14.1*	6	<0.01
Passive power per cycle (W kg^{-1})‡	–8.3±4.6	4	–17.8±15.2	4	0.28
Total power at 15% strain (W kg^{-1})	10.1±11.5	5	–14.7±13.1	6	<0.01

T_{max}, time to peak force; T_{50off}, time to 50% relaxation; T_{90off}, time to 90% relaxation; V_{max}, maximum shortening velocity.
Values are means ± s.d.
*These 179 data were previously published (Ahn and Full, 2002).
†*In vivo* strain and stimulation conditions determined during running.
‡*In vivo* strain conditions during running.

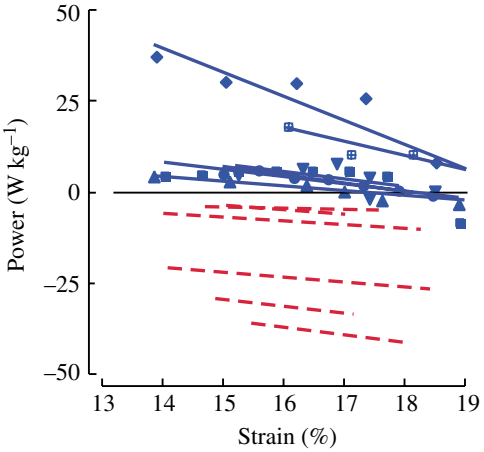

Fig. 3. Muscle power as a function of strain amplitude for muscles 178 and 179. Muscle power decreased with increasing strain for both muscles. The blue filled symbols and solid lines represent the data and regressions for muscle 178. The red broken lines represent the regression lines fitted to the data for muscle 179. Each line represents a different animal. Mechanical function for muscle 178 varied with the strain amplitude, while muscle 179 functioned to absorb energy at all strains. Data for muscle 179 have been previously published (Ahn and Full, 2002) and are presented for direct comparison with data for muscle 178.

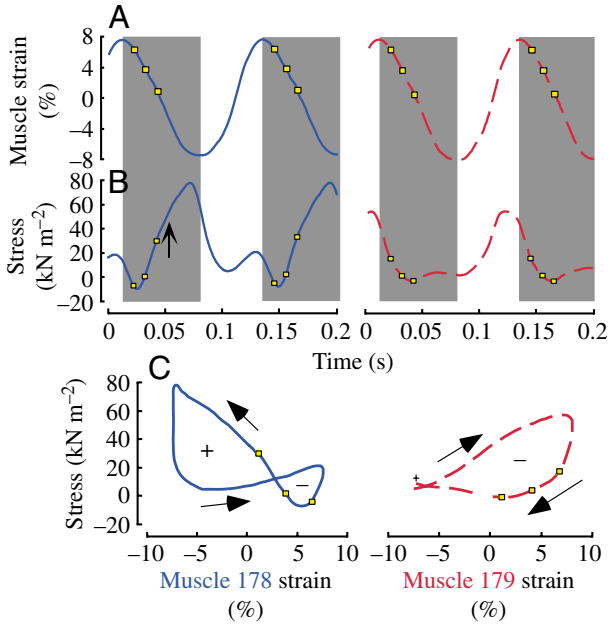

Fig. 4. Representative strain, total stress and power when muscles 178 and 179 operated under identical strain and stimulation conditions. The shaded area represents the shortening phase of the oscillatory cycle. The stimulation pattern, represented on the graphs by the yellow squares, was determined during running at the animal's preferred speed (3 pulses at 100 Hz) (Full et al., 1998; Ahn and Full, 2002). (A) The strain pattern was identical for both muscles (15% strain amplitude). (B) Muscle stress during imposed running conditions. The shaded areas represent the shortening (or stance) phase of the oscillatory cycle. (C) Work loops for muscles 178 and 179 under identical conditions. Work loops show muscle 178 generated net mechanical power during the cycle, while muscle 179 absorbed net mechanical power under identical conditions. Arrows indicate the direction of the loops.

absorption over the cycle. In muscle 179, energy absorbed during lengthening exceeded the energy generated during shortening at all strain amplitudes (Fig. 3) (Ahn and Full, 2002).

The mechanical functions of muscles 178 and 179 also differed when experiencing identical strain and stimulation conditions throughout the range of strain amplitudes examined. For example, at a strain amplitude of 15%, identical strain and stimulation inputs resulted in two very different mechanical outputs (Fig. 4). Muscle 178 generated net mechanical power over a cycle (10.1±11.5 W kg^{-1}; N=5; Table 1). By contrast, under identically imposed conditions, muscle 179 absorbed net mechanical energy over a cycle (–14.7±13.1 W kg^{-1}; N=6). In muscle 178, force increased as the muscle shortened. Force quickly declined as the muscle began to lengthen, and then force increased again as the muscle continued to lengthen. By contrast, muscle 179 generated higher force during lengthening than during shortening. Muscle 179, thereby absorbed more mechanical energy than it generated over the cycle, resulting in net energy absorption during the cycle. This difference in force generation during shortening resulted in virtually opposite mechanical functions from the two muscles during the cyclic contractions with identically imposed strain and stimulation patterns (Fig. 4).

Isometric contractions

The isometric contraction kinetics did not differ between muscles 178 and 179 (Table 1). Time to peak force generation (T_{max}), time to 50% relaxation (T_{50off}), and time to 90% relaxation (T_{90off}) during isometric twitch contractions were similar between the two muscles (Table 1). The contraction kinetics were also similar between muscles 178 and 179 when stimulated with the *in vivo* 3s activation pattern (Table 1).

Force–velocity relationships

The force–velocity relationships of muscles 178 and 179 did not differ significantly (Fig. 5). Although muscle 178 measured shorter in length than muscle 179, both muscles shortened equally fast. Absolute V_{max} for 178 (19.9±3.8 mm s^{-1}; N=5) was very similar to the absolute V_{max} for 179 [20.6±3.0 mm s^{-1} (Ahn and Full, 2002); P=0.76]. When normalized for length, the maximal rates of shortening of the two muscles were also similar (Table 1; P=0.11).

Tetanic force–length relationships

The maximum, active, tetanic force–length relationships did not differ significantly between the two muscles (Fig. 6). Optimal length, or the length of maximal force generation, occurred at 8.5±2.1% strain for muscle 178 (N=5) and 10.9±3.1% strain for muscle 179 (N=5; P=0.18). At *RL* (zero strain), each muscle generated an average of 89% of the force generated at the optimal length.

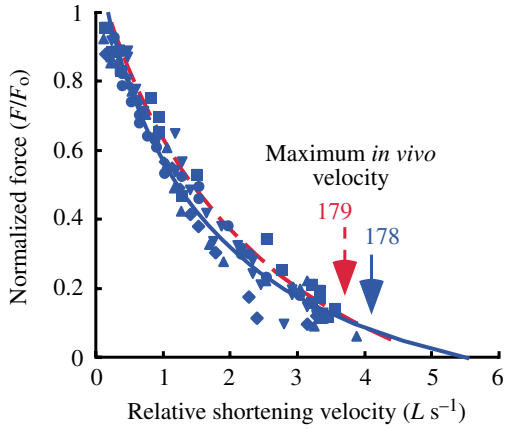

Fig. 5. Normalized force–velocity relationships for muscles 178 and 179. The normalized force–relative shortening velocity relationships did not differ between muscles 178 (filled, blue symbols) and 179 (red broken line). The solid blue line represents the curve fitted to the data for muscle 178 using the Hill equation. The arrow indicates the maximum shortening velocity experienced by both muscles when cyclically contracting at 15% strain. Different symbol shapes represent different individuals. The broken, red line representing the curve fit using the Hill equation for muscle 179 is presented for comparison (Ahn and Full, 2002).

The static, passive forces at the different muscle lengths were very low compared to the active forces (Fig. 6). Muscle 178 generated passive forces that were 1.6% of the maximum force generated by the muscle, while muscle 179 generated passive forces that were 0.8% of the maximum force.

Submaximal force–length relationships

For both muscles 178 and 179, the submaximally stimulated force–length relationships differed from the tetanic force–length relationships. Submaximal levels of stimulation (twitch and 3s stimulation levels) resulted in lower forces generated than did maximal or tetanic stimulation at all muscle lengths examined (Fig. 7A,B). Since measurements could not be obtained at lengths beyond +10% strain, 'optimal length' always referred to the length at which maximum force was generated during tetanic contractions for each muscle (see Materials and methods).

Force–length relationships when using the *in vivo* 3s stimulation pattern tended to differ between the two muscles (Fig. 7C; N=4 animals for each muscle). In maximally

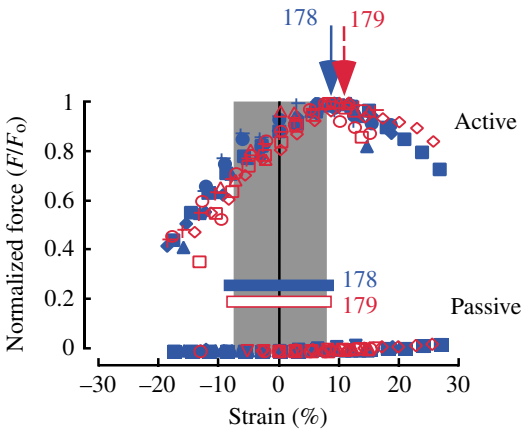

Fig. 6. Tetanic force–length relationships for muscles 178 and 179. Different symbol shapes represent different individuals. The solid blue arrow indicates optimal length for muscle 178 (filled, blue symbols), while the broken red arrow indicates optimal length for muscle 179 (open, red symbols). The region of grey shading represents the range of strains used by the muscles when cyclically oscillated at a strain amplitude of 15%. The filled and open horizontal bars span the ranges of strain experienced by the muscles under *in vivo* running conditions.

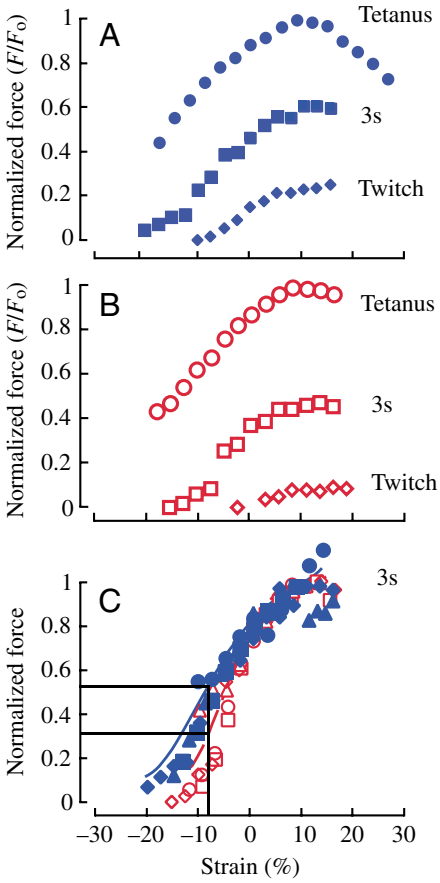

Fig. 7. Force–length relationship using the *in vivo* stimulation pattern. Representative force–length relationships for muscles 178 (A) and 179 (B). The force–length relationships at all three different stimulation levels were obtained from some individuals. (C) Forces normalized to the 3s force at the optimal length determined from the tetanic force–length relationships of muscles 178 (solid blue symbols) and 179 (open red symbols). Forces were normalized to the force at the optimal lengths determined from the tetanic force–length relationships (8.5% strain for muscle 178 and 10.9% strain for muscle 179). Fourth-order polynomial curves were fit to the combined data for muscle 178 (bold, solid blue line; R^2=0.95) and muscle 179 (red, broken line; R^2=0.96). N=4 animals for each muscle. The bold, black lines represent the difference in isometric force generated by the two muscles at –8% strain, which both muscles experience *in vivo* (see Results).

stimulated muscle, force at rest length equaled 89% of the force at optimal length for both muscles. In submaximally stimulated muscle, however, force at *RL* equaled 82% and 72% of the force at optimal length for muscles 178 and 179, respectively. As muscle length decreased, the difference in the force generated between the muscles increased. For example, at –8 and –9% strain, muscle 178 generated 67% and 87% more force than muscle 179, respectively (Fig. 7C).

Force depression due to active shortening

Force depression due to active shortening may play an important role in determining muscle force generation *in vivo* since these muscles were activated at the beginning of the stance phase of running as the muscles began shortening (Fig. 2). Under idealized conditions, force depression due to active shortening increased linearly with the magnitude of shortening strain in both muscles (Figs 8, 9). The relationships between force depression and strain did not differ between the two muscles (N=5 for each muscle; P=0.81). Following shortening strains up to 15% and when stimulated with the 3s pattern, active shortening depressed force by as much as 80% in the muscles (Fig. 9).

Force depression due to active shortening did not vary with initial length and shortening velocity in both muscles (N=5 for each muscle). While holding the shortening strain (2.5% or 0.5 mm) and shortening velocity (100 mm s^{-1}) constant, the initial length was varied up to *RL*+3 mm, which approximates 8–9% strain, in the muscles. No difference existed in the relationships of force depression and initial length between the two muscles (P=0.08), even though a statistical difference may have been observed with a larger sample size. Moreover, while holding the initial *RL* and the magnitude of shortening constant (2.5% or 0.5 mm), no difference existed between the relationships of force depression and shortening velocity between the two muscles (P=0.91).

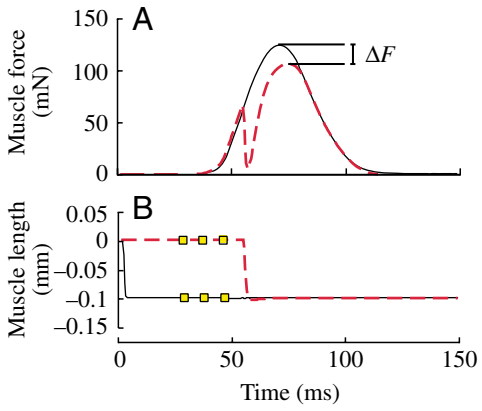

Fig. 8. Force depression due to active shortening in muscle 179. (A) Force plotted as a function of time. The solid black line represents the control contraction generated at the shorter length. The broken red line represents force with a shortening ramp generated during the contraction in muscle 179. 'ΔF' indicates the force depression or the percentage difference between the peak force of an isometric contraction held at the final, shortened length and the peak force of a contraction with active shortening. In this representative trial, active shortening (broken, red line) depressed the force generated by 16% as compared to the force generated during the control contraction (solid, black line). (B) Muscle length and stimulation (yellow squares) plotted as a function of time of the shortening contraction (broken, red line) compared with the control contraction (solid, black line).

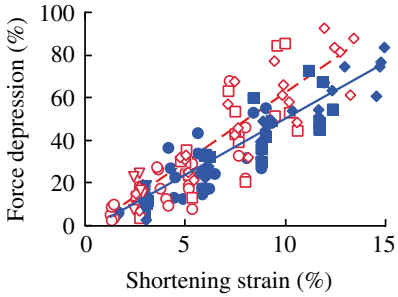

Fig. 9. Effect of strain on force depression due to active shortening in muscles 178 (filled, blue symbols) and 179 (open, red symbols). The solid blue line represents a regression of the data for muscle 178 (force depression=–0.01+4.90×strain, R^2=0.64; P<0.0001), whereas the broken red line represents a regression of the data for muscle 179 (force depression=–0.93+5.22×strain, R^2=0.56; P<0.0001). Each type of symbol represents a different initial length (circles, rest length; squares, *RL*+1 mm; diamonds, *RL*+2 mm; triangles, *RL*+3 mm). The muscles were shortened at 100 mm s^{-1} and stimulated with the 3s pattern. N=5 animals for each muscle.

Force depression due to active shortening with increasing stimulation levels decreased similarly in the two muscles (N=5 for each muscle; P=0.99). The greatest stimulation level examined matched the longest activation pattern measured in the animal during running (4 pulses of stimulation) (Ahn and Full, 2002). At this stimulation level, force depression was minimal in both muscles (3.0±4.1% for muscle 178 and 11.6±15.3% for muscle 179) for an active shortening strain of 2.5%. When stimulated with the *in vivo* 3s pattern, force depression due to active shortening in muscle 178 (11.9±4.1%; N=13) approximated that in muscle 179 (12.6±3.8%; N=9; P=0.70).

Force enhancement due to passive pre-stretch

Force enhancement due to a passive pre-stretch may play an important role in determining muscle force generation *in vivo* because these muscles are passively stretched during the swing phase prior to the stance phase of running (muscle shortening) and the onset of activation (Fig. 2). The effect of a passive stretch prior to an isometric contraction (i.e. passive pre-stretch) on force generation was independent of the magnitude of passive pre-stretch and did not differ between muscles 178 and 179 (P=0.87; Figs 10, 11). The large amount of variability in the data resulted in statistically similar isometric force generated with a passive pre-stretch relative to the force generated without a passive pre-stretch.

Stimulation level influenced force enhancement similarly between the two muscles (P=0.21). However, a twitch stimulus resulted in variation in force enhancement that ranged from 1

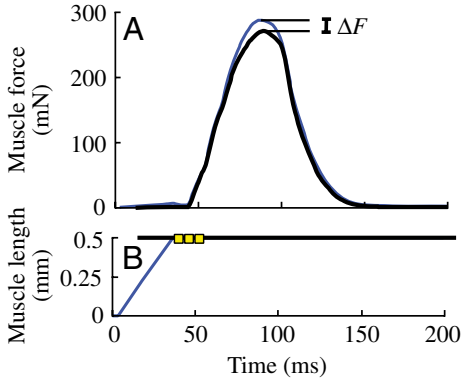

Fig. 10. Force enhancement due to passive pre-stretch in muscle 178. (A) Force plotted as a function of time. The thin black line represents the force measured in muscle 178 when stimulated isometrically at the longer length and serves as the control. The thick blue line represents the force measured in muscle 178 when stretched just prior to an isometric contraction. Force traces are aligned with respect to the stimulation to show the change in force with and without a passive pre-stretch. In this representative trial, the passive pre-stretch (thin, black line) enhanced the force generated by 6% as compared to the force generated during the control contraction (bold, blue line). (B) Muscle length and stimulation (yellow squares) plotted as a function of time of the contraction with the passive pre-stretch (thick, blue line) compared with the control contraction (thin, black line).

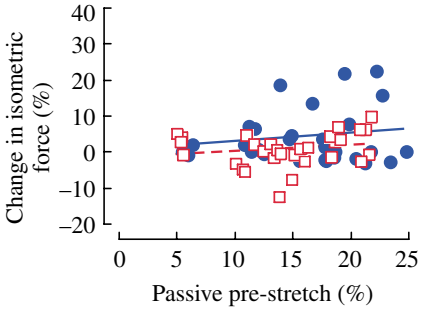

Fig. 11. Change in force as a function of passive pre-stretch for both muscles. Positive values of force enhancement represent a larger isometric force following a passive stretch. A negative value of force enhancement represents a depression following a passive stretch. The solid, blue points and line represent the data and regression for muscle 178, respectively (force change=1.35+0.20×strain; R^2=0.28; P=0.35). The open red points and broken line represent force change for muscle 179 (force change=–2.62+0.25×strain; R^2=0.065; P=0.18). As stretch distance increased, the variation in force response increased. However, the changes in force in response to a passive stretch were independent of stretch distance in both muscles. For these data, the muscles were stretched at 15 mm s^{-1}, and stimulated with the 3s pattern. N=4–7 animals for each muscle at each absolute distance of stretch.

to 100% (N=5). Very small amounts of force enhancement or depression due to passive pre-stretch resulted in large percentage changes in force output because the control twitch forces were extremely low. In contrast, when operating at the *in vivo* 3s stimulation level, force enhancement significantly differed between the muscles (P=0.005; unpaired t-test). Passive pre-stretch enhanced force in muscle 178 by 5.7±3.8% (N=6), whereas force in muscle 179 changed by –0.5±1.7% (N=6) with the same passive pre-stretch. Under the other stimulation conditions (1, 2 and 4 stimuli), no significant differences existed in force generated after a passive pre-stretch between the muscles.

Force enhancement due to passive pre-stretch did not vary with the velocity of pre-stretch in either muscle. Although the relationships of force enhancement and pre-stretch velocity were similar between muscles (ANCOVA; P=0.47), Student's unpaired t-tests showed statistical differences in force change due to passive pre-stretch between the two muscles at each of the slower pre-stretch velocities (5, 10 and 15 mm s^{-1}, at which P<0.05; N=6 at each condition for each muscle). At the fastest velocity of passive pre-stretch (100 mm s^{-1}), force enhancement did not differ between the two muscles (P=0.27; N=5 for each muscle).

Discussion

Basic muscle properties did not explain the difference in mechanical behaviours

Contrary to our initial hypothesis, two extensor muscles innervated by the same motor neuron resulted in different mechanical outputs under both *in vivo* and identical strain and stimulation conditions (Figs 2, 4). This difference in mechanical energy during cyclical contractions between muscles 178 and 179 was not caused by differences in their commonly measured properties, such as isometric contraction kinetics, tetanic force–length properties or force–velocity relationships. Their kinetics of isometric twitch and tetanic contractions, passive and maximum tetanic force–length relationships, and force–velocity properties were similar (Table 1; Figs 5, 6). Although muscle 178 measured 22% shorter in length than muscle 179, both muscles were capable of shortening equally fast. Moreover, both muscles operated at similar regions of their force–velocity relationships near V_{max} (Fig. 5). Yet, the same input conditions at 15% strain resulted in opposite net mechanical outputs from the two muscles because muscle 178 generated greater forces during shortening than muscle 179 (Fig. 4).

A previous study of insect muscle also shows that two muscles operating at a single joint can function differently (Ahn and Full, 2002). When comparing muscles 177c and 179 in the cockroach hindlimb, muscle 177c was found to generate mechanical energy and muscle 179 to absorb mechanical energy under *in vivo* running conditions (Ahn and Full, 2002). Muscles 177c and 179, however, differ greatly in length with muscle 177c measuring more than 2× longer than muscle 179. Even though the normalized force–velocity relationships are similar between the two muscles, a substantial difference in muscle length causes the two muscles to operate at different regions of their force–velocity relationships during *in vivo* strain conditions [fig. 3 in Ahn and Full (Ahn and Full, 2002)]. Muscle 177c generates more mechanical energy by operating closer to 1/3V_{max} compared to muscle 179, which operates

closer to V_{max}, under *in vivo* running conditions. That the muscles examined in the present study (178 and 179) operate on different portions of their force–velocity relationships does not explain why these muscles function differently under *in vivo* or identical conditions (Fig. 5).

Different submaximal force–length properties

Less frequently examined effects of submaximal stimulation on force production may contribute to the difference in power output during cyclical contractions between muscles 178 and 179. Although the force–length relationships of the two muscles are similar when tetanically stimulated, their relationships differ significantly at short lengths (<*RL*, Fig. 7C) when the muscles were stimulated submaximally using the *in vivo* 3s pattern. During cyclical contractions, muscle 178 generated its greatest force at the end of shortening when the muscle was shortest in length. Under identical conditions, muscle 178 generated 58% greater force than muscle 179 at –7.5% strain during submaximally stimulated isometric contractions, whereas muscle 179 generated almost no force at the end of shortening (Figs 2, 4). This observed difference in submaximal force production accounts for approximately 75% of the difference in active force generated during the oscillatory contractions with a strain amplitude of 15% (±7.5% strain) in muscles 178 and 179. The difference in force-generating capability at the lower strains explains most of the difference in force output at short lengths during dynamic contractions between the two muscles.

Submaximal stimulation, often studied using variable calcium levels, non-linearly influences force–length and force–velocity relationships of muscle (Rack and Westbury, 1969; Joyce et al., 1969; Stephenson and Wendt, 1984; deHaan, 1998; Brown et al., 1999), and their importance to the mechanical function of muscle during locomotion remains unclear. Several possible underlying mechanisms may contribute to generating differences in the submaximal force–length relationships between the two muscles. First, if muscles 178 and 179 were composed of myofilaments of different lengths, their submaximal force–length relationships would differ. However, the two muscles most likely do not have filaments of different lengths because their tetanic force–length relationships are similar (Fig. 6). Therefore, the possible mechanisms determining different submaximal force–length relationships are length-dependent, but likely not filament-dependent. For instance, these differences may be due to length-dependent differences in Ca^{2+} release or length-dependent differences in Ca^{2+} affinity to the regulatory protein (for a review, see Stephenson and Wendt, 1984).

Alternatively, differences in the interfilament spacing, which determines force generation, may result in differences in force generation at short muscle lengths between the two muscles (Bagni et al., 1990; Fuchs and Wang, 1996). Since a muscle ‘bulges’ laterally as it shortens, the space between the thin and thick filaments increases. This increase in lateral spacing between the filaments reduces the Ca^{2+} sensitivity by the myofilaments of cardiac and skeletal muscle fibres (Fuchs and Wang, 1996; Wang and Fuchs, 2000) and subsequently decreases the force generated in frog skeletal fibres (Bagni et al., 1990). If the lateral interfilament spacing in muscles 178 and 179 were to change differently in the two muscles as they shortened, then the corresponding changes in Ca^{2+} sensitivity would alter force generation differently between the two muscles. These changes in Ca^{2+} sensitivity would be smaller during maximal stimulation, however, because the higher levels of Ca^{2+} release would counter the effects of reduced Ca^{2+} sensitivity in maximal, tetanic contractions (Ekelund and Edman, 1982). Nevertheless, the two muscles likely bulge similarly as they shorten, since their strains and densities are similar.

Force depression due to active shortening

Recent studies show that force depression due to active shortening may play an important, but unclearly defined, role in the determination of mechanical function in muscles (Askew and Marsh, 1998; Josephson and Stokes, 1999; Ahn and Full, 2002; Meijer, 2002). The lack of integration that exists between isolated single fibre measurements of force depression and *in vivo* properties of whole muscle function is partly due to the controversy that surrounds the mechanism of shortening-induced force depression and partly due to the lack of relevant *in vivo* ranges of strain and stimulation conditions for animal behaviors.

Despite the near complete depression of force generated due to active shortening at *in vivo* strains in muscles 178 and 179, this history-dependent property likely does not contribute to the difference in mechanical functions during oscillatory contractions between the two muscles (Figs 2, 4). Furthermore, the magnitude of strain experienced by each muscle during locomotion (18.5% for muscle 178 and 16.4% for muscle 179; Fig. 2) was too large to obtain reliable measurements of force depression after active shortening (Fig. 9) (Edman, 1975; Herzog and Leonard, 1997; Josephson and Stokes, 1999). Nevertheless, when extrapolating to the *in vivo* strains, the force depression experiments would predict a 91% depression of the force generated by muscle 178 at 18.5% strain and an 85% depression of force generated by muscle 179 at 16.4% strain (Fig. 9). Although an active shortening of 15% strain depresses force generated by muscle 178 by 73%, a force enhancement appears to exceed this depression during cyclical contractions (arrow in Fig. 4B). In contrast, a 78% force depression due to active shortening in muscle 179 may account for the lack of force generated during the shortening phase of the oscillatory contractions at 15% strain (Fig. 4). Shortening deactivation can also have long-lasting effects (Edman, 1975; Herzog and Leonard, 1997; Josephson and Stokes, 1999), which may explain the depression of force after the end of shortening during oscillatory contractions in muscle 179.

The majority of research on force depression induced by active shortening again has relied on studies of tetanically stimulated or maximally activated muscle. In maximally stimulated muscles, force depression most often varies linearly with the magnitude of shortening (Edman, 1975; Marechal and

Plaghki, 1979; Herzog and Leonard, 1997; deRuiter et al., 1998; Herzog et al., 1998; Josephson and Stokes, 1999; Meijer, 2002), except during *in vivo*, voluntary contractions in human knee extensors (independent relationship) (Lee et al., 2000). Although force depression in submaximally stimulated frog and rat muscles does not vary with distance shortened (Colomo et al., 1986; Meijer, 2002), both submaximally stimulated insect muscles 178 and 179 show positive linear relationships between force depression and distance shortened (Fig. 9). Moreover, submaximally stimulated insect and rat muscles exhibit no effect of the initial length on force depression (see Results) (Meijer, 2002), which differs from the positive correlation in tetanically stimulated muscles (Brown and Loeb, 2000; Edman, 1980; Edman et al., 1993; Josephson and Stokes, 1999). Additionally, although shortening velocity does not influence force depression in frog fibres (Edman, 1975), *in vivo* knee extensors of humans (Lee et al., 2000) and insect muscle (see Results), they negatively correlate for the majority of the muscles examined (Marechal and Plaghki, 1979; Herzog and Leonard, 1997; Josephson and Stokes, 1999; deRuiter and deHaan, 2003). Stimulation level also generally negatively correlates with force depression [see Results (Ekelund and Edman, 1982; Edman et al., 1993); up to 50 Hz in crab muscle (Josephson and Stokes, 1999); rat muscle (Meijer, 2002)]. However, stimulation level has no effect on force depression due to active shortening *in vivo* in the human thumb muscle (deRuiter et al., 1998; deRuiter and deHaan, 2003) and in the cat caudofemoralis muscle (Brown and Loeb, 2000). Although the number of studies examining shortening-induced force depression continues to increase, few general relationships have yet to emerge.

Effects of passive pre-stretch

As expected from the cyclical contractions, greater levels of force enhancement induced by a passive pre-stretch occurred in muscle 178 than in muscle 179, but only slightly and not under all the conditions. A pre-stretch enhanced force by 6% more in muscle 178 than in muscle 179 under conditions closest to those observed *in vivo* during running (0.5 mm pre-stretch; 15 mm s^{-1}; 3s stimulation pattern). This difference in force enhancement between the two muscles accounts for about 10% of the force difference observed during cyclical contractions. Passive ramp stretches also enhance the isometric force in slow- but not fast-twitch muscle in rats (Mutungi and Ranatunga, 2001). However, the implications of force enhancement due to passive pre-stretch in vertebrates are unknown because the functional effects of passive pre-stretch on force generation have not yet been examined using dynamic contractions.

Implications for mechanical power output during locomotion

By selecting animals with the simplest possible neural wiring, we discovered that the mechanical function of a muscle during locomotion cannot necessarily be predicted from anatomical position, neural activation patterns and kinematics alone or in concert, even when isometric contraction kinetics, force–velocity properties and force–length properties were similar. Differential effects of submaximal stimulation may influence the mechanical function of muscles *in vivo*. These differences in mechanical output under *in vivo* conditions may function to allow one muscle to modulate its function. With slight changes in activation or strain conditions, muscle 178 is capable of functioning like a motor to generate net mechanical power or like a brake to absorb net mechanical energy (Fig. 3) depending on the mechanical demands. On the other hand, muscle 179 likely functions like a brake under most *in vivo* conditions without the capacity for modulation in function. Predicting muscle function during locomotion requires an integrative approach from whole body locomotion to the measurement of non-traditional muscle properties.

Determination of basic or commonly measured muscle properties, including twitch contraction kinetics, force–length and force–velocity properties, appears insufficient to explain muscle behaviour during locomotion (Josephson, 1999; Sandercock and Heckman, 1997; Perreault et al., 2003). Under the dynamic conditions of running, swimming or flying, muscles do not operate as they would when maximally stimulated, held isometrically or shortened isotonically. Differences between the two leg muscles in their observed submaximal force–length relationships account for approximately 75% of the difference between the two muscles in peak force generated at short lengths during oscillatory contractions (Figs 4, 7). Using the *in vivo* conditions of the muscles to examine their submaximal force-generating properties provides clues to how muscles could function differentially during running in this animal. Many muscles in animals undergo cyclic, submaximally stimulated contractions during motor behaviours as diverse as running, flying, swimming, breathing and chewing. Understanding the functional consequences of shortening deactivation, stretch activation and submaximal stimulation under such widespread functional conditions can reveal differences in force generation that are not apparent during maximally stimulated isometric and isotonic experiments of muscle.

List of abbreviations

3s	3 pulses of stimulation at 100 Hz
EMG	electromyographical
RL	rest length or length of the muscle when the coxal–trochanteral–femoral joint was positioned at a 90° angle
T_{max}	time to peak force of an isometric contraction
T_{50off}	time to 50% relaxation of an isometric contraction
T_{90off}	time to 90% relaxation of an isometric contraction
V_{max}	maximal rate of shortening of muscle

The authors thank A. Biewener, S. Lehman, R. Monti, G. Gillis, C. Farley and M. Koehl for comments on earlier drafts of the manuscript. We also thank two anonymous reviewers

for their helpful comments. Special thanks to M. H. Dickinson for use of his stimulation isolation unit and E. Chen for Fig. 1A. This research was supported by ONR Grant N00014-92-J-1250 AASERT Award, Sigma Xi Grants-In-Aid of Research, Department of Integrative Biology Summer Fellowship, and NIH F32 AR47741 to A.N.A.

References

Ahn, A. N. and Full, R. J. (2002). A motor and a brake: two leg extensor muscles acting at the same joint manage energy differently in a running insect. *J. Exp. Biol.* **205**, 379-389.

Askew, G. N. and Marsh, R. L. (1998). Optimal shortening velocity (V/V_{max}) of skeletal muscle during cyclical contractions: length–force effects and velocity-dependent activation and deactivation. *J. Exp. Biol.* **201**, 1527-1540.

Bagni, M. A., Cecchi, G. and Colomo, F. (1990). Myofilament spacing and force generation in intact frog muscle fibres. *J. Physiol.* **430**, 61-75.

Becht, G., Hoyle, G. and Unsherwood, P. N. R. (1960). Neuromuscular transmission in the coxal muscles of the cockroach. *J. Insect Physiol.* **4**, 191-201.

Brown, I. E. and Loeb, G. E. (2000). Measured and modeled properties of mammalian skeletal muscle. III. The effects of stimulus frequency on stretch-induced force enhancement and shortening-induced force depression. *J. Muscle Res. Cell Motil.* **21**, 21-31.

Brown, I. E., Cheng, E. J. and Loeb, G. E. (1999). Measured and modeled properties of mammalian skeletal muscle. II. The effects of stimulus frequency and force-velocity relationships. *J. Muscle Res. Cell Motil.* **20**, 627-643.

Carbonell, C. S. (1947). The thoracic muscles of the cockroach *Periplaneta americana. Smith. Misc. Coll.* **107**, 1-23.

Colomo, F., Lombardi, V. and Piazzesi, G. (1986). A velocity-dependent shortening depression in the development of the force-velocity relation in frog muscle fibres. *J. Physiol.* **380**, 227-238.

deHaan, A. (1998). The influence of stimulation frequency on force–velocity characteristics of *in situ* rat medial gastrocnemius muscle. *Exp. Physiol.* **83**, 77-84.

deRuiter, C. J. and deHaan, A. (2003). Shortening-induced depression of voluntary force in unfatigued and fatigued human adductor pollicis muscle. *J. Appl. Physiol.* **94**, 69-74.

deRuiter, C. J., deHaan, A., Jones, D. A. and Sargeant, A. J. (1998). Shortening-induced force depression in human adductor pollicis muscles. *J. Physiol.* **507**, 583-591.

Dickinson, M. H., Farley, C. T., Full, R. J., Koehl, M. A. R., Kram, R. and Lehman, S. (2000). How animals move: an integrative view. *Science* **288**, 100-106.

Edman, K. A. P. (1975). Mechanical deactivation induced by active shortening in isolated muscle fibres of the frog. *J. Physiol.* **246**, 255-275.

Edman, K. A. P. (1979). The velocity of unloaded shortening and its relation to sarcomere length and isometric force in vertebrate muscle fibres. *J. Physiol.* **291**, 143-159.

Edman, K. A. P. (1980). Depression and mechanical performance by active shortening during twitch and tetanus of vertebrate muscle fibres. *Acta Physiol. Scand.* **109**, 15-26.

Edman, K. A. P., Caputo, C. and Lou, F. (1993). Depression of tetanic force induced by loaded shortening of frog muscle fibres. *J. Physiol.* **466**, 535-552.

Ekelund, M. C. and Edman, K. A. P. (1982). Shortening induced deactivation of skinned fibres of frog and mouse striated muscle. *Acta Physiol. Scand.* **116**, 189-199.

Fuchs, F. and Wang, Y. P. (1996). Sarcomere length versus interfilament spacing as determinants of cardiac myofilament Ca^{2+} sensitivity and Ca^{2+} binding. *J. Mol. Cell. Cardiol.* **28**, 1375-1383.

Full, R. J. and Ahn, A. N. (1995). Static forces and moments generated in the insect leg: comparison of a three-dimensional musculo-skeletal computer model with experimental measurements. *J. Exp. Biol.* **198**, 1285-1298.

Full, R. J., Blickhan, B. and Ting, L. H. (1991). Leg design in hexapedal runners. *J. Exp. Biol.* **158**, 369-390.

Full, R. J., Stokes, D. R., Ahn, A. N. and Josephson, R. K. (1998). Energy absorption during running by leg muscles in a cockroach. *J. Exp. Biol.* **201**, 997-1012.

Herzog, W. and Leonard, T. R. (1997). Depression of cat soleus forces following isokinetic shortening. *J. Biomech.* **30**, 865-572.

Herzog, W., Leonard, T. R. and Wu, J. Z. (1998). Force depression following skeletal muscle shortening is long lasting. *J. Biomech.* **31**, 1163-1168.

Josephson, R. K. (1985). Mechanical power output from striated muscle during cyclic contraction. *J. Exp. Biol.* **114**, 493-512.

Josephson, R. K. (1999). Dissecting muscle power output. *J. Exp. Biol.* **202**, 3369-3375.

Josephson, R. K. and Stokes, D. R. (1999). Work-dependent deactivation of a crustacean muscle. *J. Exp. Biol.* **202**, 2551-2565.

Joyce, G. C., Rack, P. M. H. and Westbury, D. R. (1969). The mechanical properties of cat soleus muscle during controlled lengthening and shortening movements. *J. Physiol.* **204**, 461-474.

Ker, R. F. (1977). Some structural and mechanical properties of locust and beetle cuticle. PhD thesis, University of Oxford, UK.

Lee, H. D., Suter, E. and Herzog, W. (2000). Effects of speed and distance of muscle shortening on force depression during voluntary contractions. *J. Biomech.* **33**, 917-923.

Marechal, G. and Plaghki, L. (1979). The deficit of the isometric tetanic tension redeveloped after a release of frog muscle at a constant velocity. *J. Gen. Physiol.* **73**, 453-467.

Meijer, K. (2002). History dependence of force production in submaximal stimulated rat medial gastrocnemius muscle. *J. Electromyogr. Kinesiol.* **12**, 463-470.

Morgan, C. R., Tarras, M. S. and Stokes, D. R. (1980). Histochemical demonstration of enzymatic heterogeneity within the mesocoxal and metacoxal muscles of *Periplaneta americana*. *J. Insect Physiol.* **26**, 481-486.

Mutungi, G. and Ranatunga, K. W. (2001). The effects of ramp stretches on active contractions in intact mammalian fast and slow muscle fibres. *J. Muscle Res. Cell Motil.* **22**, 175-184.

Pearson, K. G. and Iles, J. F. (1971). Innervation of coxal depressor muscles in the cockroach *Periplaneta americana*. *J. Exp. Biol.* **54**, 215-232.

Perreault, E. J., Heckman, C. J. and Sandercock, T. G. (2003). Hill muscle model errors during movement are greatest within the physiologically relevant range of motor unit firing rates. *J. Biomech.* **36**, 211-218.

Pipa, R. L. and Cook, E. F. (1959). Studies on the hexapod nervous system. I. The peripheral distribution of the thoracic nerves of the adult cockroach, *Periplaneta americana*. *Ann. Entomol. Soc. Am.* **52**, 695-710.

Rack, P. M. H. and Westbury, D. R. (1969). The effects of length and stimulus rate on tension in the isometric cat soleus muscle. *J. Physiol.* **204**, 443-460.

Sandercock, T. G. and Heckman, C. J. (1997). Doublet potentiation during eccentric and concentric contractions of cat soleus muscle. *J. Appl. Physiol.* **82**, 1219-1228.

Stephenson, D. G. and Wendt, I. R. (1984). Length dependence of changes in sarcoplasmic calcium concentration and myofibrillar calcium sensitivity in striated muscle fibres. *J. Muscle Res. Cell Motil.* **5**, 243-272.

Stokes, D. R. (1987). Insect muscles innervated by single motoneurons: structural and biochemical features. *Am. Zool.* **27**, 1001-1010.

Stokes, D. R., Vitale, A. J. and Morgan, C. R. (1979). Enzyme histochemistry of the mesocoxal muscles of *Periplaneta americana*. *Cell Tissue Res.* **198**, 175-189.

Usherwood, P. N. R. (1962). The nature of 'slow' and 'fast' contractions in the coxal muscles of the cockroach. *J. Insect Physiol.* **8**, 31-52.

Wang, Y. P. and Fuchs, F. (2000). Length-dependent effects of osmotic compression on skinned rabbit psoas muscle fibers. *J. Muscle Res. Cell Motil.* **21**, 313-319.

Wohlfart, B. and Edman, K. A. P. (1994). Rectangular hyperbola fitted to muscle force-velocity data using three-dimensional regression analysis. *Exp. Physiol.* **79**, 235-239.